A-

W. G. Davey - Idaho - Bldg. 774

May 26, 1971

FRA-TM-13

EVALUATION OF SPACE-ENERGY FACTORIZATION FOR TWO-DIMENSIONAL LMFBR DIFFUSION THEORY PROBLEMS

Weston M. Stacey, Jr.

Argonne National Laboratory
Applied Physics Division
9700 South Cass Avenue
Argonne, Illinois 60439

FRA TECHNICAL MEMORANDUM NO. 13

Results reported in the FRA-TM series of memoranda frequently are preliminary and subject to revision. Consequently they should not be quoted or referenced without the author's permission.

Work performed under the auspices of the U. S. Atomic Energy Commission.

Evaluation of Space-Energy Factorization for Two-Dimensional LMFBR Diffusion Theory Problems

Weston M. Stacey, Jr.
Applied Physics Division, Argonne National Laboratory
Argonne, Illinois 60439

Use of a space-energy factorization (SEF) scheme to obtain approximate solutions to the energy-dependent neutron diffusion equation was suggested in Ref. 1, where the method was successfully applied to one-dimensional/24-group LMFBR models. Initial applications of the method to two-dimensional/24-group and one-dimensional/165-group LMFBR models were reported in Ref. 2. The purpose of this note is to report the results of subsequent numerical studies undertaken to evaluate the efficacy of the method for two-dimensional/24-group LMFBR models.

SEF has been incorporated into the inner iteration to obtain an approximate solution to

$$H(r,E)\phi(r,E) = \int_E^\infty dE' \, K(r,E' \to E) \, \phi(r,E') + S(r,E) \tag{1}$$

by factoring the flux within each of several shape function intervals $E_g \leq E \leq E_{g+1}$ in the form

$$\phi(r,E) \simeq a(E)\psi_g(r) \ , \quad E_g \leq E \leq E_{g+1} \ . \tag{2}$$

Substituting relation (2) into Eq. (1) and integrating over the interval $E_g \leq E \leq E_{g+1}$ yields equations for the shape functions, ψ_g

$$\left[\int_{E_g}^{E_{g+1}} dE\ H(r,E)a(E)\right]\psi_g(r) = \int_{E_{g'}}^{E_{g+1}} dE\ S(r,E)$$

$$+ \sum_{g' \leq g}\left[\int_{E_g}^{E_{g+1}} dE \int_{E_g}^{E_{g'+1}} dE'\ K(r,E' \rightarrow E)a(E')\right]\psi_{g'}(r)\ , \tag{3}$$

and the same substitution together with an integration over space yields an equation for the spectral function, a(E),

$$\left[\int dr\ H(r,E)\psi_g(r)\right]a(E) = \int dr\ S(r,E)$$

$$+ \sum_{g' \leq g}\int_{E_{g'}}^{E_{g'+1}} dE'\left[\int dr\ K(r,E' \rightarrow E)\psi_{g'}(r)\right]a(E')\ . \tag{4}$$

In a typical calculation reported in this note, employing six shape-function intervals, Eq. (4) would be solved on a 24-group basis for a(E). The interval $E_g \leq E \leq E_{g+1}$ would contain 4 of the 24 groups, thus Eqs. (3) would be solved on a 6 broad-group basis.

On each inner iteration, ψ_1 from the previous inner iteration is used to evaluate the spatial integrals in Eq. (4). Then a(E), $E_1 \leq E \leq E_2$, is obtained by solving Eq. (4), and used to evaluate the energy integrals over this interval in Eqs. (3). Then Eq. (3) is solved for ψ_1. This

value of ψ_1, and ψ_2 from the previous inner iteration, are used to evaluate the spatial integrals in Eq. (4), which is solved for a(E), $E_2 \leq E \leq E_3$. This value of a(E) is used to evaluate the energy integrals over this interval in Eqs. (3), which are then solved for ψ_2. This process is repeated for all shape function intervals.

The solution of Eqs. (3), which are formally identical to the multigroup equations, is accomplished iteratively with an ADI-B^2 method similar to that of Ref. 3. Equation (4), which is identical to the fundamental mode slowing-down equation, is solved directly.

Power iteration, with two-term Chebyschev extrapolation, was employed for the outer iterations. One inner iteration per outer iteration was used (i.e. the SEF procedure outlined above was used once each outer iteration, and a single sweep in each direction was used in solving Eq. (3) by the ADI-B^2 scheme). Numerical experiments revealed that the spectral function, a(E), did not change much from iteration to iteration after the first few iterations. Accordingly, the spectral function was recalculated each iteration for the first five iterations, and subsequently only recalculated every fifth outer iteration. For the direct 24-group solution the same iteration scheme was used (i.e. power iteration with two-term Chebyschev extrapolation on the outer), so that a meaningful evaluation of the computational savings associated with the SEF method could be made.

Numerical studies of the SEF method were performed on three reactor models typical of proposed LMFBRs. The geometric model is shown in Fig. 1 (for Model 3 the X-dimensions were 50, 40, 40, and 10 cm), and the compositions are given in Table I. Model 1 is very similar to models which have been used in preliminary design studies for LMFBRs. Model 2 value of ψ_1, and ψ_2 from the previous inner iteration, are used to evaluate the spatial integrals in Eq. (4), which is solved for $a(E)$, $E_2 \le E \le E_1$. This value of $a(E)$ is used to evaluate the energy integrals over this interval in Eqs. (3), which are then solved for ψ_2. This process is repeated for all shape function intervals.

The solution of Eqs. (3), which are formally identical to the multigroup equations, is accomplished iteratively with an ADI-B^2 method similar to that of Ref. 3. Equation (4), which is identical to the fundamental mode slowing-down equation, is solved directly.

Power iteration, with two-term Chebyschev extrapolation, was employed for the outer iterations. One inner iteration per outer iteration was used (i.e. the SEF procedure outlined above was used once each outer iteration, and a single sweep in each direction was used in solving Eq. (3) by the ADI-B^2 scheme). Numerical experiments revealed that the spectral function, $a(E)$, did not change much from iteration to iteration after the first few iterations. Accordingly, the spectral function was recalculated each iteration for the first five iterations, and subsequently only recalculated every fifth outer iteration. For the direct N-group solution the same iteration scheme was used (i.e. power iteration with two-term Chebyschev extrapolation on the outers), so that a meaningful evaluation of the computational savings associated with the SEF method could be made.

Numerical studies of the SEF method were performed on three reactor models typical of proposed LMFBRs. The geometric model is shown in Fig. 1 (for Model 3 the X-dimensions were 50, 40, 40, and 10 cm), and the compositions are given in Table I. Model 1 is very similar to models which have been used in preliminary design studies for LMFBRs. Model 2 differs from Model 1 only in that the sodium has been completely voided from Core 2 and Axial Blanket 2, and represents a hypothetical accident condition. Model 3 was chosen to provide a more difficult test of the SEF method; the sodium content in the two core regions is significantly different and a significant amount of plutonium has been included in the blankets.

The objectives of these studies were to evaluate the accuracy and computational economy of the SEF method, particularly relative to the similar but simpler few-group approximations obtained by group collapsing, and to evaluate the efficacy of using the fission source from the SEF solution as an initial guess to accelerate the convergence of direct 24-group solutions. The few-group constants were obtained by collapsing over a critically buckled 24-group spectrum for the composition of Core 1.

Results shown in Table II indicate that the SEF method is significantly more accurate in the prediction of criticality than a few-group method which employs the same number of spatial-shape calculations. Callations with only two shape functions are significantly more accurate than two-group calculations in predicting the maximum power peaking, and the six-shape function calculation is somewhat superior to the six-group calculation in this respect. Regional power fractions are predicted better by the two-shape function calculation than by the two-group calculation, but there is little difference between the six-shape function and six-group predictions, as indicated in Tables III-V. Power distributions along the horizontal and vertical centerlines of Model 3 are shown in Figs. 2 and 3.

For Models 1 and 2 the few-group predictions of breeding ratios are somewhat better than the corresponding SEF predictions, due to compensating

errors in the few-group calculations which predict too hard a spectrum and too much flux in the blankets. This trend is reversed for Model 3. These results are shown in Tables III-V.

The computation times and number of outer iterations associated with the various calculations are shown in Table VI. The two-shape function calculation is roughly a factor of 5 quicker than the direct solution, and the six-shape function solution, which is quite accurate, is roughly a factor of 3 quicker than the direct solution. Few group solution times are 20-30% less than the corresponding shape function solution times. The computation of the collapsing spectrum and the preparation of the few-group constants has not been included in the former, but this will not significantly alter the comparison.

Use of the fission source from the SEF calculation as a first guess in the direct 24-group solution significantly reduces (25-40%) both the number of iterations and the total computing time relative to what is required when the standard flat fission source is used as a first guess. In this respect, use of the two-shape function solution is more economical than use of the more accurate six-shape function solution. Use of the fission source from the few-group calculations may also reduce the computing time required for the 24-group calculation, but this point has not been investigated.

In summary, the SEF method provides an economical means for obtaining approximate solutions to two-dimensional LMFBR diffusion theory problems. These solutions are sufficiently accurate for many applications, and generally superior to the results of comparable few-group calculations. Moreover, use of the SEF solution to accelerate the direct solution can significantly reduce the computational time for the latter. Thus, it errors in the few-group calculations which predict too hard a spectrum and too much flux in the blankets. This trend is reversed for Model 3. These results are shown in Tables III-V.

The computation times and number of outer iterations associated with the various calculations are shown in Table VI. The two-shape function calculation is roughly a factor of 5 quicker than the direct solution, and the six-shape function solution, which is quite accurate, is roughly a factor of 3 quicker than the direct solution. Few group solution times are 10-30% less than the corresponding shape function solution times. The computation of the collapsing spectrum and the preparation of the few-group constants has not been included in the former, but this will not significantly alter the comparison.

Use of the fission source from the SEF calculation as a first guess in the direct 24-group solution significantly reduces (25-40%) both the number of iterations and the total computing time relative to what is required when the standard flat fission source is used as a first guess. In this respect, use of the two-shape function solution is more economical than use of the more accurate six-shape function solution. Use of the fission source from the few-group calculations may also reduce the computing time required for the 24-group calculation, but this point has not been investigated.

In summary, the SEF method provides an economical means for obtaining approximate solutions to two-dimensional LMFBR diffusion theory problems. These solutions are sufficiently accurate for many applications, and generally superior to the results of comparable few-group calculations. Moreover, use of the SEF solution to accelerate the direct solution can significantly reduce the computational time for the latter. Thus, it seems appropriate to conclude that the capability of multidimensional diffusion theory codes designed to solve 20- to 30-group LMFBR problems could be substantially enhanced by providing for the SEF calculation. The necessary modifications should be minor, because Eqs. (3) can be solved by the same routines which solve the conventional multigroup equations and the solution of Eq. (4) is trivial. The strategy outlined above for the SEF method is consistent with the group-ordering stategy employed in many diffusion theory codes, so no major changes in data management should be necessary.

REFERENCES

[1]W. M. STACEY, JR., "Solution of the Neutron Diffusion Equations by Space-Energy Factorization," *Nucl. Sci. Eng.*, to be published; also FRA-TM-3, Argonne National Laboratory (1970).

[2]W. M. STACEY, JR., and H. HENRYSON, II, "Applications of Space-Energy Factorization to the Solution of Static Fast-Reactor Neutronics Problems," *Proc. Conf. New Developments in Reactor Mathematics and Applications, Idaho Falls, March 1971,* The American Nuclear Society to be published; also FRA-TM-11, Argonne National Laboratory (1971).

[3]L. A. HAGEMAN and J. B. YASINSKY, "Comparison of Alternating Direction Time-Differencing Methods with Other Implicit Methods for the Solution of the Neutron Group-Diffusion Equations," *Nucl. Sci. Eng.*, 38, 8 (1969).

TABLE I

Compositions

	Atomic Number Densities (at/cc × 10^{24})					
	Core 1	Core 2	Axial Blanket 1	Axial Blanket 2	Radial Blanket	Reflector
			Models 1 and 2[a]			
^{239}Pu	0.001086	0.001501	---	---	---	---
^{238}U	0.006383	0.005380	0.008013	0.007383	0.014515	---
^{23}Na	0.01041	0.01098	0.00881	0.00950	0.00660	0.00440
^{56}Fe	0.01814	0.01807	0.02444	0.02385	0.01728	0.06912
^{16}O	0.01494	0.01376	0.01603	0.01477	0.02903	---
			Model 3			
^{239}Pu	0.0009	0.0013	0.0002	0.0001	0.0003[b]	---
^{238}U	0.0055	0.0048	0.0070	0.0070	0.0111[b]	---
^{23}Na	0.0120	0.0080	0.0100	0.0070	0.0060[b]	0.0040
^{56}Fe	0.0180	0.0180	0.0240	0.0240	0.0170	0.0690
^{16}O	0.0150	0.0140	0.0160	0.0150	0.0290	---

TABLE II

Errors in k_{eff} and Maximum Power Peaking

Calculation	k_{eff} (% Error)			P_{max} (% error)		
	Model 1	Model 2	Model 3	Model 1	Model 2	Model 3
2 SF	-0.8	-0.2	-0.6	+1.1	+0.1	-0.8
4 SF	-0.2	---	---	+0.5	---	---
6 SF	+0.1	+0.3	+0.1	+0.4	-0.6	+0.6
2-group	+1.2	+1.2	-6.5	-3.4	-1.0	+5.6
6-group	+0.4	+0.4	-0.9	+0.7	+0.7	+1.0

TABLE II

Errors in k_{eff} and Maximum Power Peaking

Calculation	k_{eff} (% Error)			P_{max} (% error)		
	Model 1	Model 2	Model 3	Model 1	Model 2	Model 3
2 SF	-0.8	-0.2	-0.6	+1.1	+0.1	-0.8
4 SF	-0.2	---	---	+0.5	---	---
6 SF	+0.1	+0.3	+0.1	+0.4	-0.6	+0.6
2-group	+1.2	+1.2	-6.5	-3.4	-1.0	+5.6
6-group	+0.4	+0.4	-0.9	+0.7	+0.7	+1.0

TABLE III

Breeding Ratio and Power Fraction, Model 1

Calculation	Breeding Ratio[c]					Power Fraction (%)			
	Total	Axial Blanket	Radial Blanket	Core 1	Core 2	Axial Blanket	Radial Blanket	Core 1	Core 2
24-group	1.164	0.305	0.206	0.499	0.154	1.3	1.3	64.6	32.8
2 SF	1.109	0.260	0.190	0.496	0.164	2.6	2.4	62.3	32.7
4 SF	1.131	0.280	0.195	0.498	0.158	1.7	1.6	63.9	32.8
6 SF	1.136	0.287	0.196	0.496	0.156	1.4	1.3	64.3	33.0
2-group	1.118	0.265	0.196	0.495	0.162	3.0	2.7	62.1	32.2
6-group	1.143	0.289	0.199	0.498	0.157	1.4	1.3	64.3	33.0

TABLE IV

Breeding Ratio and Power Fraction, Model 2

Calculation	Breeding Ratio[c]					Power Fraction (%)			
	Total	Axial Blanket	Radial Blanket	Core 1	Core 2	Axial Blanket	Radial Blanket	Core 1	Core 2
24-group	1.025	0.316	0.063	0.493	0.153	1.4	0.6	63.9	34.1
2 SF	0.943	0.263	0.045	0.476	0.159	2.8	0.7	62.5	34.0
6 SF	0.994	0.295	0.058	0.488	0.153	1.5	0.6	64.3	33.6
2-group	0.970	0.273	0.045	0.490	0.162	3.2	0.7	62.5	33.6
6-group	1.014	0.302	0.059	0.496	0.158	1.5	0.6	63.8	34.1

Table V

Breeding Ratio and Power Fraction, Model 3

Calculation	Breeding Ratio[c]					Power Fraction (%)			
	Total	Axial Blanket	Radial Blanket	Core 1	Core 2	Axial Blanket	Radial Blanket	Core 1	Core 2
24-group	1.062	0.285	0.227	0.347	0.203	9.1	4.8	42.9	43.2
2 SF	1.027	0.257	0.210	0.344	0.216	9.5	5.6	41.5	43.4
6 SF	1.044	0.274	0.217	0.347	0.206	8.9	4.7	43.0	43.4
2-group	1.024	0.248	0.198	0.350	0.228	8.3	4.5	41.6	45.6
6-group	1.037	0.271	0.213	0.346	0.206	8.8	4.8	43.0	43.5

TABLE VI

Computational Times and Iterations

Calculation	Model 1		Model 2		Model 3	
	No. Iterations	min[d]	No. Iterations	min[d]	No. Iterations	min[d]
24-group	15	10.90	15	11.26	15	8.87
2 SF	15	2.05	17	1.98	15	1.76
6 SF	16	3.10	16	3.23	14	2.48
2-group	15	---	15	1.39	15	1.23
6-group	15	---	15	2.53	15	1.99
24-group/2 SF[e]	7	7.05	7	7.24	7	5.90
24-group/6 SF[e]	7	8.10	--	---	6	6.03

TABLE VI

Computational Times and Iterations

Calculation	Model 1 No. Iterations	Model 1 min^d	Model 2 No. Iterations	Model 2 min^d	Model 3 No. Iterations	Model 3 min^d
24-group	15	10.30	15	11.26	15	8.87
2 SF	15	2.05	17	1.38	15	1.76
6 SF	16	3.10	16	3.23	14	2.48
7-group	15	---	15	1.39	15	1.23
6-group	15	---	15	2.53	15	1.93
24-group/2 SF^c	7	7.05	7	7.24	7	5.90
24-group/6 SF^e	7	8.10	--	---	6	6.03

Footnotes for Tables:

[a]For Model 2, the sodium number density was zero for Core 2 and Axial Blanket 2.

[b]For that portion of the radial blanket which extends above the core axially, $^{239}Pu = 0.0001$, $^{238}U = 0.0112$, $^{23}Na = 0.0070$.

[c]The breeding ratio for a region is defined as the ratio of the ^{238}U capture in that region to the ^{239}Pu absorption in the entire reactor. The total breeding ratio then results as a sum of region breeding ratios.

[d]Central Processing Unit, IBM-360-50/75.

[e]The fission source from the 2- (or 6) shape SEF calculation was used as an initial guess in the 24-group calculation. The computing time includes the time required for the SEF calculation and the time required for the 24-group calculation.

FIGURE CAPTIONS

1. Two-dimensional LMFBR model.
2. Power distribution along vertical centerline (left boundary) for Model 3.
3. Power distribution along horizontal centerline (lower boundary) for Model 3.

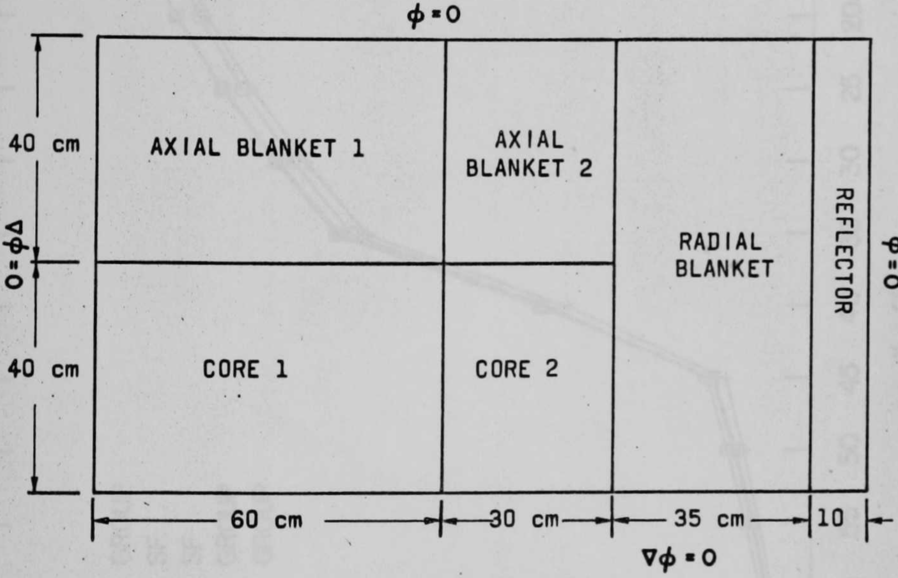

Fig. 1. Two-dimensional LMFBR model.
(ANL Neg. No. 116-634)

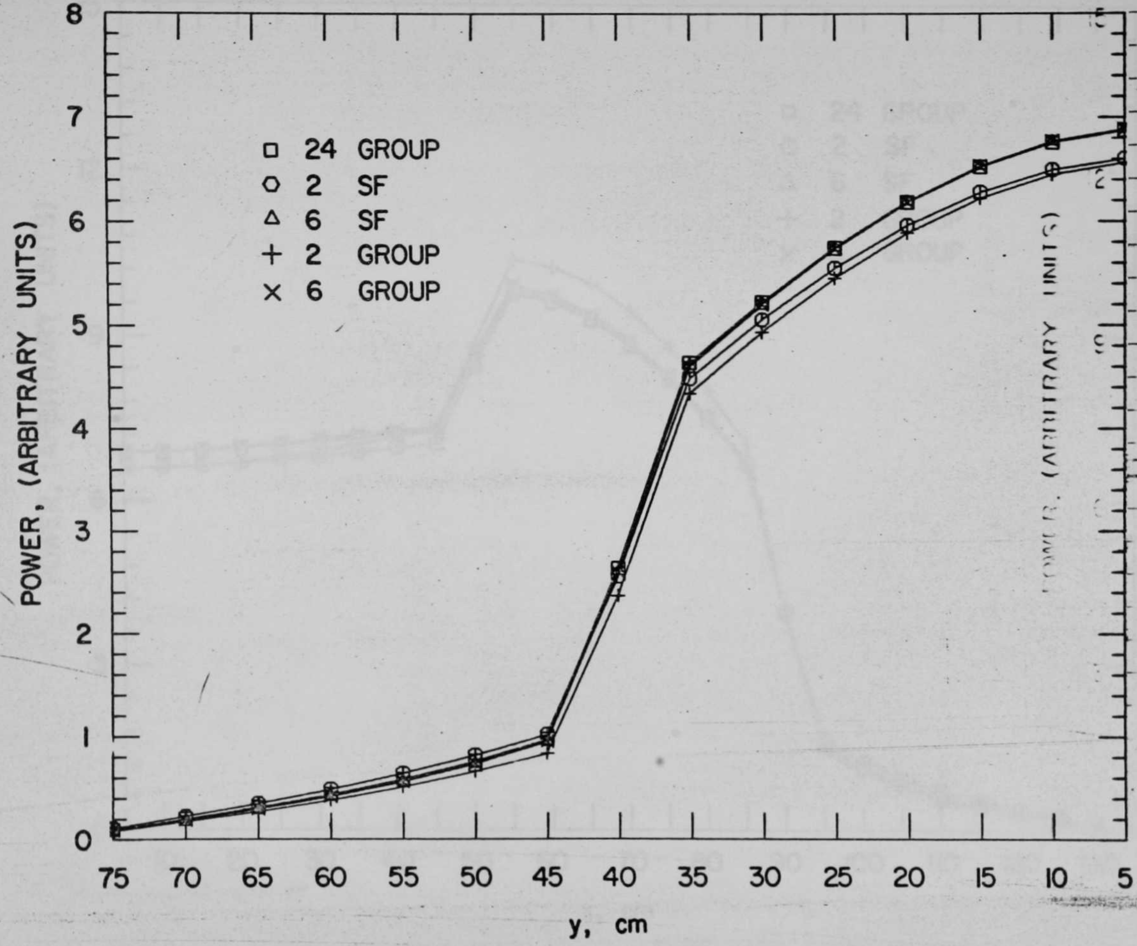

Fig. 2. Power distribution along vertical centerline (left boundary) for Model 3. (ANL Neg. No. 116-701)

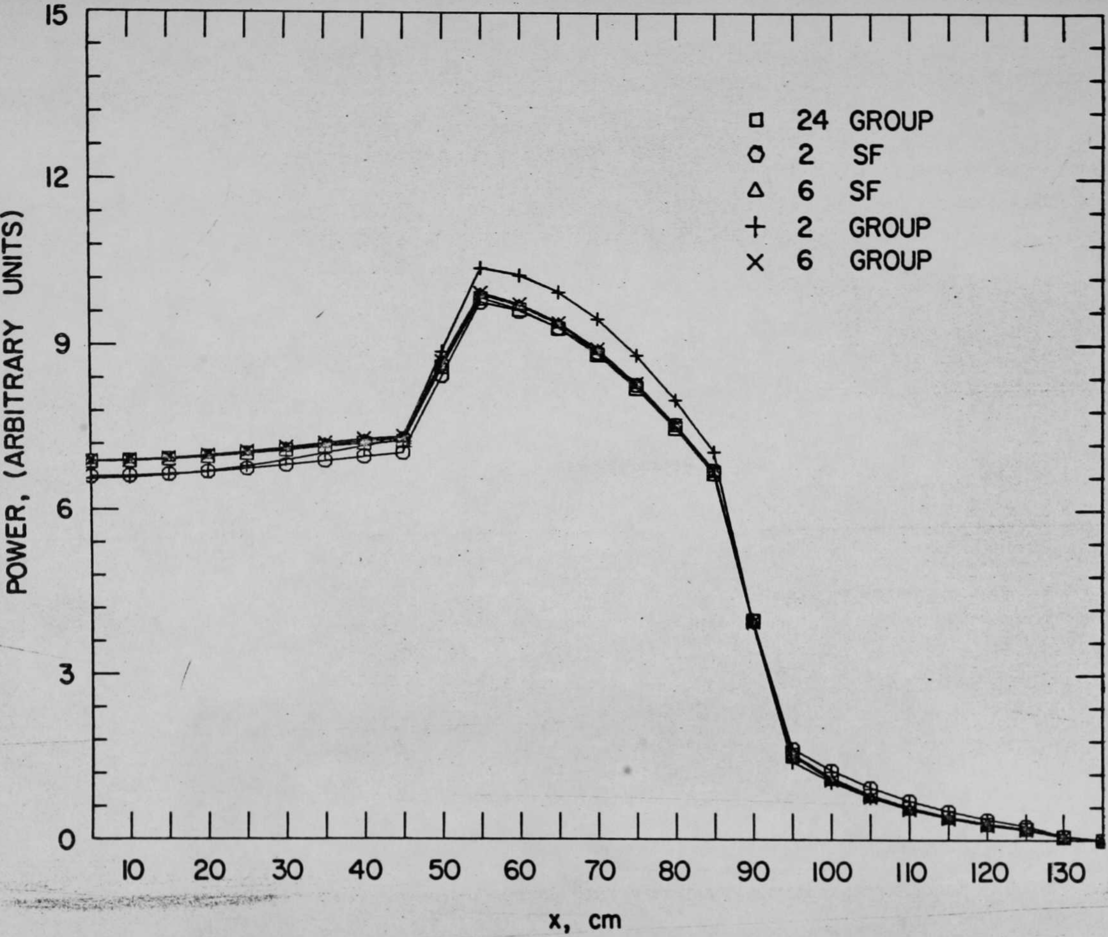

Fig. 3. Power distribution along horizontal centerline (lower boundary) for Model 3.